CHAPTER IV
RESULTS AND DISCUSSION

4.1 Adsorption of Linear Sodium Dodecylbenzene Sulfonates on Single-Walled Carbon Nanotubes

4.1.1 Aggregate Morphology of Linear Sodium Dodecylbenzene Sulfonates on Single-Walled Carbon Nanotubes

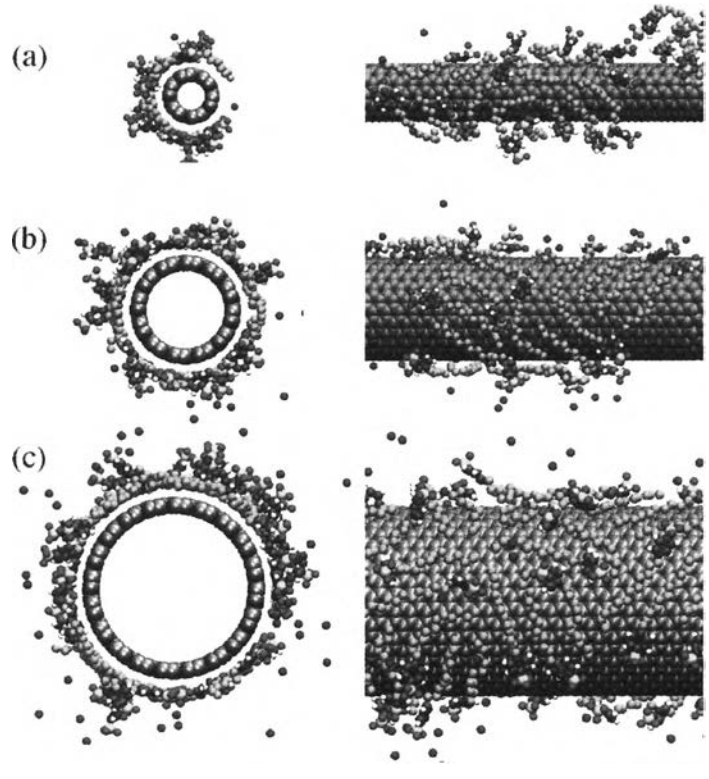

Figure 4.1 Front and side views of representative simulation snapshots of equilibrated linear SDBS surfactants adsorbed on (a) (6,6), (b) (12,12), and (c) (20,20) SWNTs at low surface coverage. Water molecules are not shown for clarity. Color code: cyan for CH_n-groups; purple for carbon atoms in benzene rings; white for hydrogen atoms in benzene rings; red for oxygen atoms; yellow for sulfur atoms; blue for sodium counterions; grey for carbon atoms in SWNTs.

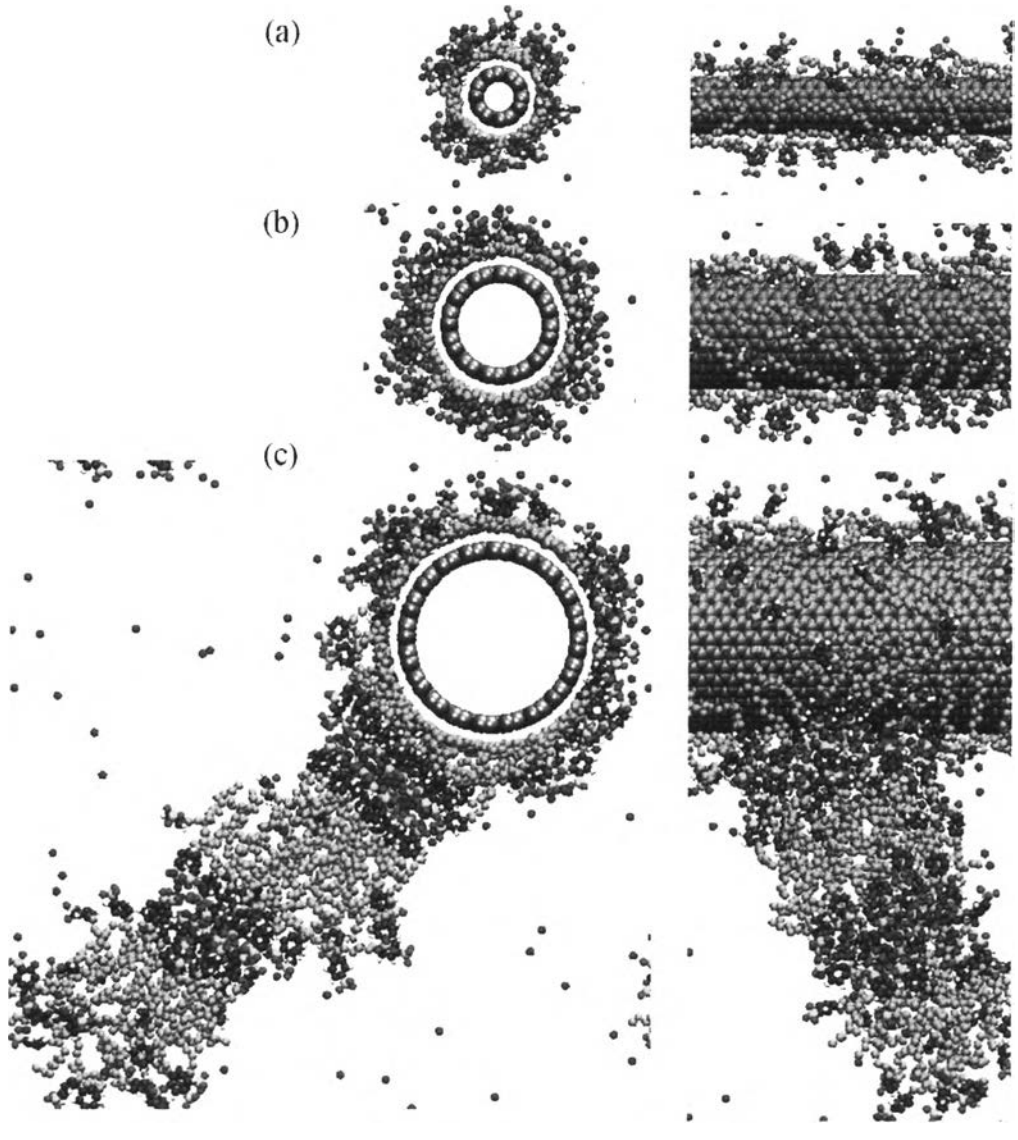

Figure 4.2 Front and side views of representative simulation snapshots of equilibrated linear SDBS surfactants adsorbed on (a) (6,6), (b) (12,12), and (c) (20,20) SWNTs at high surface coverage. Water molecules are not shown for clarity. The color code is the same as that used in Figure 4.1.

Representative simulation snapshots of linear SDBS surfactants adsorbed on (6,6), (12,12), and (20,20) SWNTs are shown in Figures 4.1 and 4.2. At low surface coverage (Figure 4.1), the snapshots show that linear SDBS molecules wrap around the SWNTs, forming a ring. The tail segments and most benzene rings are positioned closely to the SWNT surface while the sulfonate headgroups are

exposed to water. However, it is noted that, unexpectedly, some headgroups can be found near the nanotube surface.

At high surface coverage, illustrated in Figure 4.2, it is noticed that the tail segments adsorb in a compact manner around the SWNT surface. Unexpectedly, based on the argument according to which π-π interactions dictate the packing of SDBS on nanotubes, most benzene rings are found further from the nanotubes, next to the layer of tail segments. The sulfonate headgroups mainly extend toward the aqueous phase. On (20,20) SWNT, the formation of micelles adsorbed on the tubes is observed. Sodium counterions (blue spheres) can be found in between the linear SDBS headgroups within the micelle and the linear SDBS headgroups on the (20,20) SWNT, suggesting that strong counterion condensations lead to the formation of the aggregates shown in Figure 4.2.

It should be pointed out that SDBS micelles, as well as isolated SDBS monomers, were found within the aqueous phase for all systems shown in Figure 4.1 and 4.2. However, only on (20,20) SWNT it can be observed the multi-layered structure, as shown in the bottom panel of Figure 3. It is possible that as the surfactant concentrations increase within the simulated systems exotic structures such as that observed on (20,20) SWNTs form also on the other nanotubes considered, leading to surface coverages comparable to those estimated experimentally by Matarredona *et al.* (2003). As mentioned earlier, coarse-grain methods such as DPD should be implemented to study such systems (Angelikopoulos and Bock, 2009; Calvaresi *et al.*, 2009). The results presented here can be used to quantify the surfactant structure at relatively low surface coverage, focusing on those SDBS molecules that, after an extensive equilibration time, remain at contact with the nanotubes.

Focusing on the adsorbed SDBS surfactants, common feature shared by Figure 4.1 and 4.2 is that each SWNT is covered by a monolayer of linear SDBS molecules. The tail segments and the benzene rings remain in contact with the nanotube surface while the headgroups extend to the aqueous phase. Hydrophobic interactions between the tail segments and the SWNTs are responsible for these results. A great number of sodium counterions accumulate near the sulfonate groups due to the strong electrostatic attraction between the oppositely charged groups. This

feature is in good agreement with both experimental observations relative to SDBS (Islam *et al.*, 2003; Matarredona *et al.*, 2003) and simulation results for other surfactants (Lin *et al.*, 2010; Tummala and Striolo, 2009; Tumala *et al.*, 2010; Xu *et al.*, 2010).

4.1.2 Population Analysis Results for Linear Sodium Dodecylbenzene Sulfonates on Single-Walled Carbon Nanotubes

In order to quantify the effective surface coverage of linear SDBS on the three SWNTs, the time-average number of linear SDBS adsorbed on the SWNT by integrating the number density profiles of the linear SDBS molecules around the SWNT (shown later) up to a cutoff distance of 12 Å was calculated. The linear SDBS molecules located within the cutoff distance from the SWNT surface are considered to be adsorbed on the nanotube , and the linear SDBS molecules that are beyond the cutoff distance are considered as dispersed in the aqueous media (these can be found as monomers, sometimes, as small aggregates, as shown in Figure 4.3).

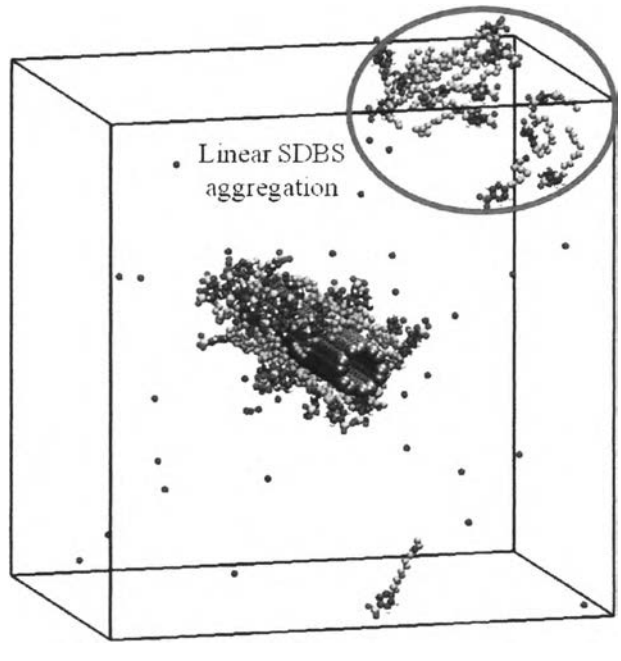

Figure 4.3 The linear SDBS aggregates considered as dispersed in the aqueous media. Water molecules are not shown for clarity. The color code is the same as that used in Figure 4.1.

The average number of SDBS not adsorbed is calculated at the difference between the total number of SDBS molecules present in the simulation box and the average number of SDBS molecules adsorbed on the nanotube. Detailed results of population analysis for linear SDBS at both low and high surface coverages are summarized in Table 4.1.

Table 4.1 Population analysis results for linear SDBS on SWNTs

Substrate	Number of SDBS	Nominal SDBS surface coverage (nm^2/headgroup)	Average number of adsorbed SDBS	Average number of non adsorbed SDBS	Effective SDBS surface coverage (nm^2/headgroup)
(6,6)	19	1.0	14.00	5.00	1.36
(12,12)	38	1.0	27.00	11.00	1.41
(20,20)	63	1.0	54.00	9.00	1.17
(6,6)	53	0.357	36.95	16.05	0.51
(12,12)	106	0.357	56.02	49.98	0.68
(20,20)	178	0.357	89.75	88.25	0.71

Despite the careful preparation of simulation boxes, it is noted from Table 4.1 that the surface coverage at both low and high coverages changes from system to system. At high surface coverage, a large number of linear SDBS molecules do not adsorbed, particularly on (12,12) and (20,20) SWNTs. As a consequence, the effective linear SDBS surface coverages considered in this study are 0.68 and 0.71 nm^2/headgroup, respectively. As the nominal surface coverage increases, the number of surfactants present within each simulation box increases, and the probability of forming micelles aggregates not adsorbed on the nanotubes also increases. This leads to much lower effective than nominal surface coverages.

4.1.3 Radial Density Profiles

Focusing on the adsorbed SDBS molecules, the positions of each SDBS fraction (tail, benzene ring, and headgroup) on the SWNTs can be quantified by calculating density distribution away from the SWNT surface. The position of surfactant tail is identified by either CH_2 or CH_3 groups in the dodecane backbone. The positions of benzene ring and headgroup are defined as the center of mass of either the benzene ring or the sulfonate group, respectively. The density distributions of tail segments, benzene rings, sulfonate headgroups, and sodium counterions on (6,6), (12,12), and (20,20) SWNTs are shown in Figure 4.4.

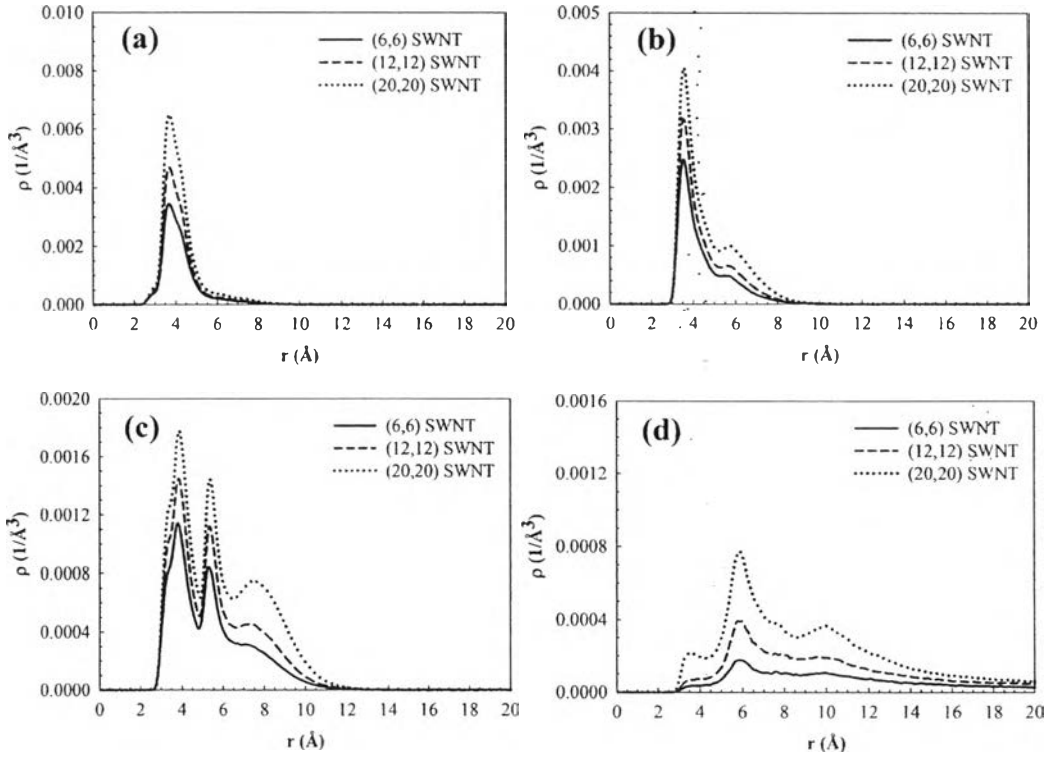

Figure 4.4 Density distribution of (a) tail segments, (b) benzene rings, (c) headgroups, and (d) sodium counterions of linear SDBS relative to the SWNT ("r" is measured radially from the nanotube surface). These results were obtained on the three SWNTs at low surface coverage. The solid, dashed, and dotted lines represent (6,6), (12,12), and (20,20) SWNTs, respectively.

The density distributions obtained on the three SWNTs at low surface coverage are illustrated in Figure 4.4. The density profile of the tail segments on the three SWNTs displays a strong peak at 3.5 Å (Figure 4.4a), indicating that the tail segments adsorb on the SWNT surface. Most benzene rings are located near the nanotube surface (Figure 4.4b). A small fraction of the benzene rings extend to water, as can be noticed from the shoulder found at ~6 Å. Since benzene groups lie on the SWNT surface, it can be observed that some of the sulfonate headgroups are located near the SWNT surface, as demonstrated by the first peak at 4 Å (Figure 4.4c). This result was unexpected because the headgroups are hydrophilic. The peak at 5.5 Å and the shoulder at 7.5 Å show that some headgroups are positioned away from the substrate towards the aqueous phase. Sodium counterions accumulate near the charged sulfonate groups with the largest peak at 6 Å (Figure 4.4d), evidence of counterion condensation (Tummala and Striolo, 2008).

As shown in Figure 4.1 and 4.2, the linear SDBS aggregate morphology is affected by surface coverage. Comparing the density profiles just discussed to those obtained at high surface coverage (Figure 4.5) leads to quantify such quantitative observations. Even at high surface coverage the tail segments (Figure 4.5a) are predominantly adsorbed on the SWNT, manifesting a strong peak at 4 Å. At high surface coverage, the benzene rings are found both close to the nanotube surface and a little further, just next to the layer of tail segments (Figure 4.5b). The density profile of benzene rings becomes wider with a thickness of around 5 Å. At high surface coverage, the results show that a majority of headgroups are predominantly found away from the SWNT surface, yielding the largest density peak at 8.5 Å (Figure 4.5c). However, a few headgroups remain near the substrate, with small density peaks at 4 and 5.5 Å, even at high surface coverage.

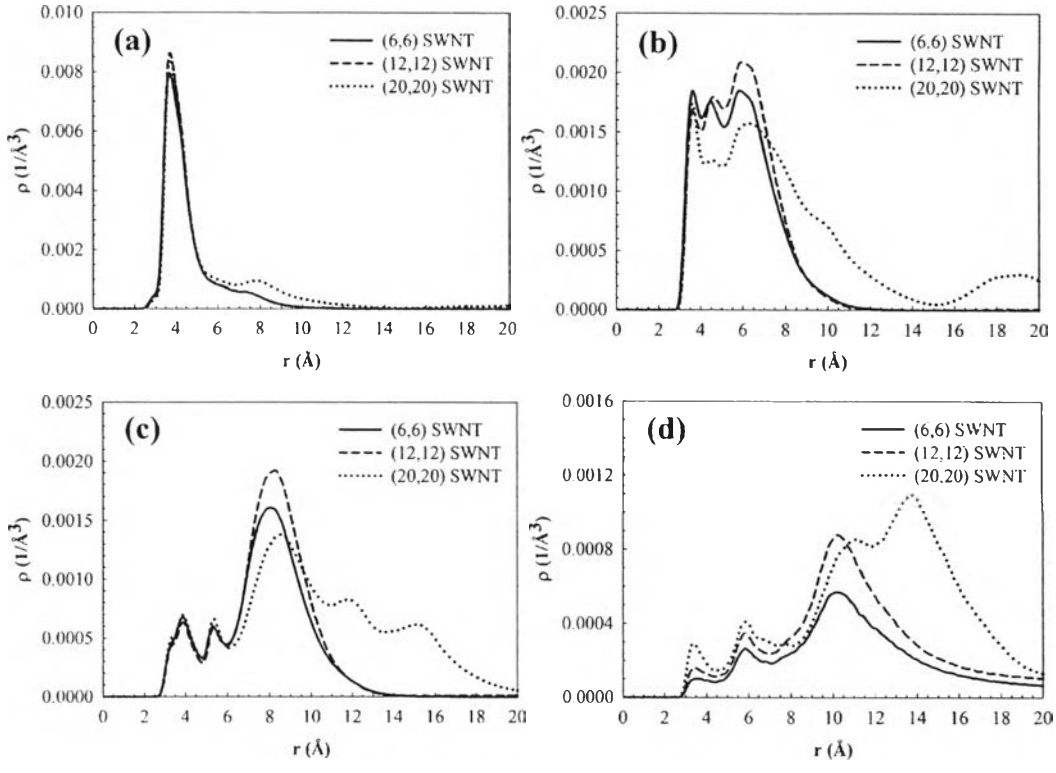

Figure 4.5 Density distribution of (a) tail segments, (b) benzene rings, (c) headgroups, and (d) sodium counterions of linear SDBS relative to the SWNT ("r" is measured radially from the nanotube surface). These results were obtained on the three SWNTs at high surface coverage. The solid, dashed, and dotted lines represent (6,6), (12,12), and (20,20) SWNTs, respectively.

In the case of (20,20) SWNT, the density profile of headgroups is quite different from that observed for (6,6) and (12,12) SWNTs. This is a consequence of the formation of the micelles at contact with the adsorbed SDBS surfactants, as shown in Figure 4.2c. Because of the micelles, a large number of headgroups can be found away from the SWNT surface and hence it can be observed the shoulder at 12 and 15 Å in the density profile. At high surface coverage, on all nanotubes, the sodium counterions associate closely to the sulfonate headgroups (Figure 4.5d). The accumulation of the positively charged counterions near the negatively charged sulfonate groups is due to counterion-condensation phenomena. The counterion condensation shields the electrostatic repulsion between the charged sulfonate groups and effectively brings them close to each other, similarly to what

has been observed in previous studies (Lin *et al.*, 2010; Tummal and Striolo, 2008; Tummala and Striolo, 2009; Tummala *et al.*, 2010).

4.1.4 Oreintation Distribution

The aggregate morphology of linear SDBS surfactants assemblies on SWNTs depend not only upon the surface coverage but also, to some extent, upon the SWNT diameter. Visual inspection of simulation snapshots suggests that on (6,6) SWNT (Figure 4.1a), the tail segments appear to lie parallel to the SWNT axis. As the SWNT diameter increases, the tail segments orient themselves both parallel and perpendicular to the nanotube axis, especially on (20,20) SWNT (Figure 4.1c). Similarly results were observed for SDS surfactants and attributed to the stiffness of the surfactant tails (Tummala and Striolo, 2009).

To quantify the orientation of linear SDBS molecules adsorbed on the three SWNTs, the angle between the vector identified by the surfactant tail and the SWNT axis, and that between the vector identified by the benzene sulfonate and the SWNT axis were calculated. Only linear SDBS molecules located up to a cutoff distance of 9 (tail) and 12 Å (sulfonate) from the SWNT surface were considered for these calculations. A schematic illustrating the two vectors defined by one SDBS molecule is shown in Figure 4.6. Note that when the angle between either the surfactant tail or the benzene sulfonate and the SWNT axis is 0° or 180°, the correspondent vector is parallel to the nanotube axis. When this angle is 90°, the vector is perpendicular to the nanotube axis.

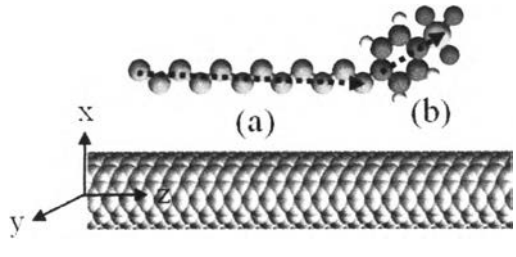

Figure 4.6 The vectors defined by (a) tail segments and (b) benzene sulfonates used to calculate the probability distribution of the orientation angle between linear SDBS molecule and the SWNT axis (parallel to the z-axis of the simulation box).

The probability distribution of the angle of linear SDBS molecules on (6,6), (12,12), and (20,20) SWNTs at low surface coverage is illustrated in Figure 4.7. In Figure 4.7a, the surfactant tail has a preference for orienting parallel to the tube axis on (6,6) and (12,12) SWNTs. On (20,20) SWNT, the tail segments tend to lie with various angles to the nanotube axis. This can be explained by considering that linear SDBS surfactant has the dodecyl chain with length on the order of 2 nm. Thus, when adsorbing onto a narrow tube, particularly (6,6) SWNT with diameter 0.814 nm, it is energetically favorable for the rigid tails to lie along the tube axis rather than to wrap around the circumference (Islam *et al.*, 2003). The probability distribution corresponding to the angle between the benzene sulfonate and the SWNT axis is shown in Figure 4.7b. One broad peak around 90° is observed on (20,20) SWNT suggesting that the sulfonate group orients preferentially perpendicularly to the tube. There is no preferential orientation of benzene sulfonate groups on (6,6) and (12,12) SWNTs. These results further confirm that the benzene rings do not lie on the nanotube surfaces, as was expected based on the π-π interactions argument (Clark *et al.*, 2011; Islam *et al.*, 2003; Tan and Resasco, 2005).

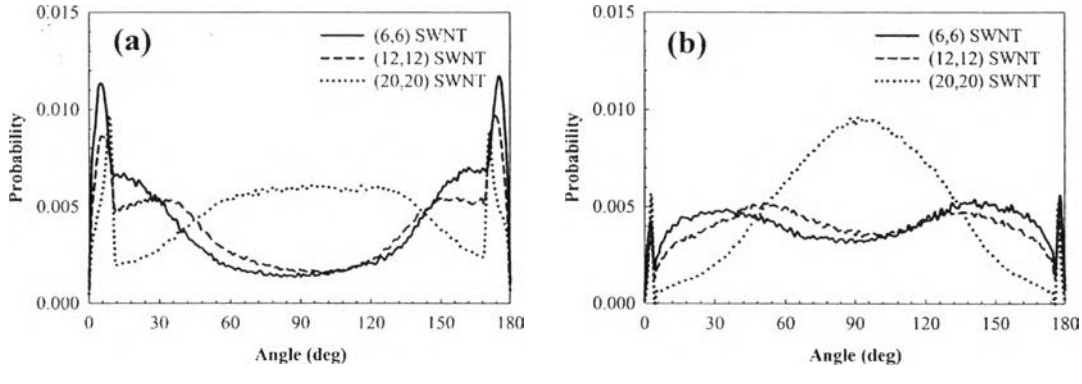

Figure 4.7 Probability distribution of orientation angle formed between the vector of the surfactant tail and the SWNT axis [(a) and (c)] and that between the vector of the benzene sulfonate and the SWNT axis [(b) and (d)]. These results were obtained on the three SWNTs at low surface coverage. The solid, dashed, and dotted lines represent (6,6), (12,12), and (20,20) SWNTs, respectively.

At high surface coverage (Figure 4.8), the surfactant tails (Figure 4.8a) do not show pronounced preferred orientation. The noticeable peaks at 0° and 180° on (6,6) SWNT suggest some preference for parallel orientation on this SWNT. In Figure 4.8b, it can be observed very broad peaks centered around 90° on (6,6) and (12,12) SWNTs, indicating that the benzene sulfonate groups tend to lie perpendicular to the nanotubes. This tendency is more pronounced on the (20,20) SWNT, where the peak at 90° is sharper. The small peaks at 0° and 180° indicate that a few benzene sulfonate groups orient parallel to SWNT axis.

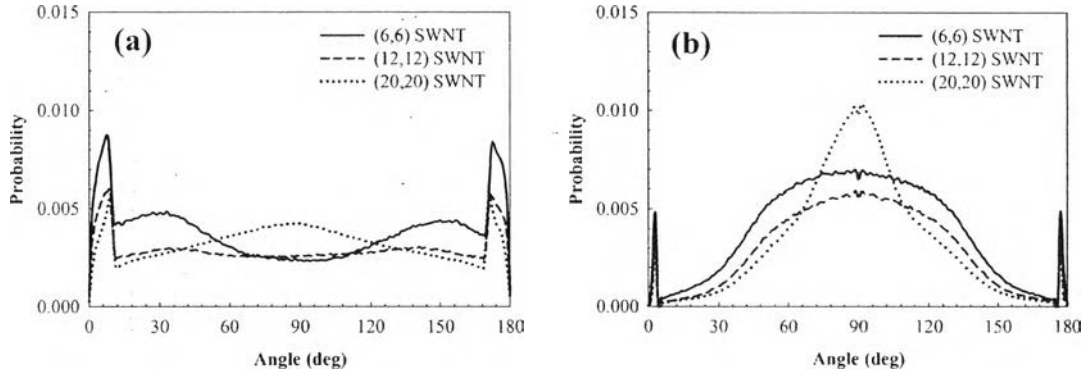

Figure 4.8 Probability distribution of orientation angle formed between the vector of the surfactant tail and the SWNT axis [(a) and (c)] and that between the vector of the benzene sulfonate and the SWNT axis [(b) and (d)]. These results were obtained on the three SWNTs at high surface coverage. The solid, dashed, and dotted lines represent (6,6), (12,12), and (20,20) SWNTs, respectively.

In all the cases discussed so far, the structures of linear SDBS aggregates formed on the SWNTs do not agree with the model for the surfactant-nanotube aggregates suggested by Matarredona *et al.* (2003). These authors proposed that the SDBS surfactants lie perpendicular to the surface taking indeed the appearance of a cylindrical micelle while the nanotube resting in the interior. Simulation results suggest that the linear SDBS aggregates are disordered at the SWNT surface. It should be remembered, however, that these simulations are conducted at low surfactant coverage. As the surfactant density increases, it is possible that multi-layered aggregates such as the one shown in Figure 4.2c are

formed. Unfortunately, atomistic MD cannot be used, within the current computational resources, to investigate such systems.

4.2 Adsorption of Branched Sodium Dodecylbenzene Sulfonates on Single-Walled Carbon Nanotubes

4.2.1 Aggregate Morphology of Branched Sodium Dodecylbenzene Sulfonates on Single-Walled Carbon Nanotubes

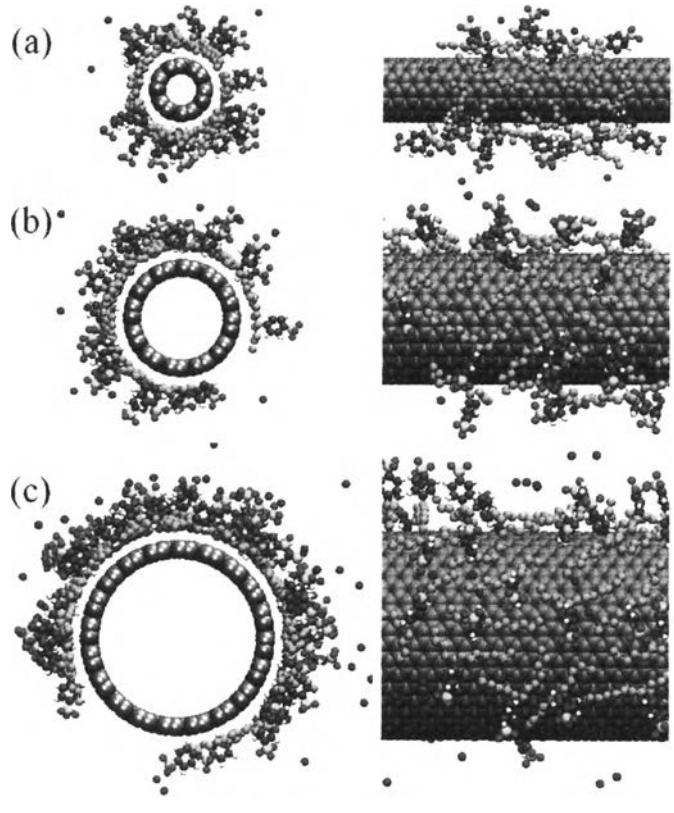

Figure 4.9 Front and side views of representative simulation snapshots of equilibrated branched SDBS surfactants adsorbed on (a) (6,6), (b) (12,12), and (c) (20,20) SWNTs at low surface coverage. Water molecules are not shown for clarity. The color code is the same as that used in Figure 4.1.

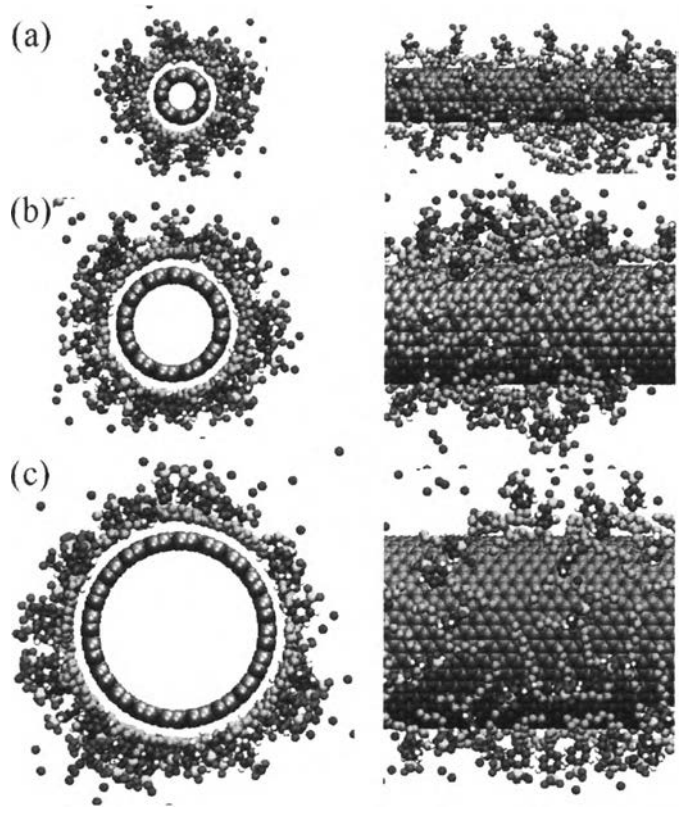

Figure 4.10 Front and side views of representative simulation snapshots of equilibrated branched SDBS surfactants adsorbed on (a) (6,6), (b) (12,12), and (c) (20,20) SWNTs at high surface coverage. Water molecules are not shown for clarity. The color code is the same as that used in Figure 4.1.

To quantify the SDBS aggregate morphology on SWNTs as a function of the SDBS molecular structure, the self-assembled aggregates formed by branched SDBS were studied at conditions comparable to those considered above. The branched SDBS molecules were obtained by grafting the benzene sulfonate to the 5^{th} carbon atom in the dodecane backbone (see Figure 3.1).

Representative simulation snapshots of branched SDBS adsorbed on (6,6), (12,12) and (20,20) SWNTs at low and high surface coverages are shown in Figure 4.9 and 4.10, respectively. Visual inspection of the simulation snapshots reveal significant qualitative differences compared to results obtained for linear SDBS at comparable surface coverages. A shared feature of snapshots in both figures is that the tail segments adsorb close to the substrates while the benzene rings are

located further from the nanotube surfaces, next to the layer of tail segments. A large number of headgroups extend to the aqueous phase.

4.2.2 Population Analysis Results for Branched Sodium Dodecylbenzene Sulfonates on Single-Walled Carbon Nanotubes

As in the case for linear SDBS, not all branched surfactants present within the various simulation boxes are found adsorbed on the SWNTs after equilibration. Integrating the number density profiles near each SWNT up to a cutoff distance of 12 Å, the number of adsorbed branched SDBS was estimated, as well as that of non adsorbed branched SDBS. The results, together with the effective surface coverage, are reported in Table 4.2.

Table 4.2 Population analysis results of branched SDBS adsorbed on SWNTs

Substrate	Number of SDBS	Nominal SDBS surface coverage (nm^2/headgroup)	Average number of adsorbed SDBS	Average number of non adsorbed SDBS	Effective SDBS surface coverage (nm^2/headgroup)
(6,6)	19	1.0	18.99	0.01	1.00
(12,12)	38	1.0	23.02	14.98	1.65
(20,20)	63	1.0	55.00	8.00	1.15
(6,6)	53	0.357	39.99	13.01	0.48
(12,12)	106	0.357	46.00	60.00	0.83
(20,20)	178	0.357	61.31	116.69	1.03

On (6,6) SWNT, the packing density of the branched SDBS molecules is higher than that obtained for linear SDBS both at low and high surface coverages. This observation may be due to the molecular structure of branched SDBS, which appears to be comparable with the diameter of (6,6) SWNT. By

contrast, on (12,12) and (20,20) SWNTs the adsorbed branched SDBS are fewer than linear SDBS. This may be due to preferential adsorption of branched SDBS on narrow SWNTs, although compelling data are not available to support this hypothesis.

4.2.3 Radial Density Profiles

As above in the case of branched SDBS, the properties of adsorbed branched SDBS were quantified, focusing on those surfactants found on the nanotubes after equilibration. The arrangements of adsorbed branched SDBS can be quantified by the density profiles of tail segments, benzene rings, headgroups, and counterions away from the SWNT surface. The density profiles of branched SDBS at low surface coverage are illustrated in Figure 4.11.

The tail segments remain in contact with the nanotube surface, as indicated by the peak around 4 Å (Figure 4.11a). Although a small portion of the benzene rings is located near the substrate, most of the benzene rings are positioned further from the SWNT surface, next to the monolayer formed by the tail segments (Figure 4.11b). The sulfonate headgroups tend to be exposed to water (Figure 4.11c). On (20,20) SWNT, it can be obtained a strong peak for the headgroup density profile at ~10 Å, indicating that headgroups are predominantly away from the nanotube suface. On all SWNTs, the sodium counterions accumulate near the headgroups due to the counterion condensations (Figure 4.11d), in qualitative agreement with results obtained for linear SDBS.

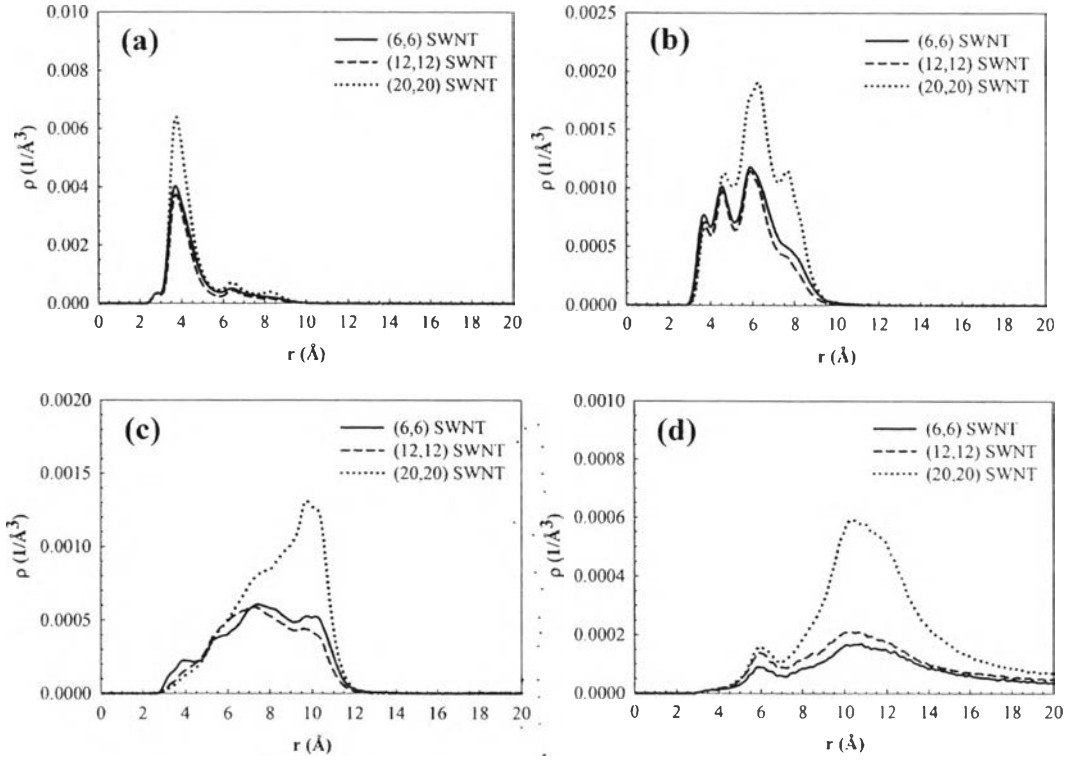

Figure 4.11 Density distribution of (a) tail segments, (b) benzene rings, (c) headgroups, and (d) sodium counterions of branched SDBS relative to the SWNT ("r" is measured radially from the nanotube surface). These results were obtained on the three SWNTs at low surface coverage. The solid, dashed, and dotted lines represent (6,6), (12,12), and (20,20) SWNTs, respectively.

The density profiles of branched SDBS at high surface coverage are shown in the right panels of Figure 4.12. The tail segments strongly adsorb on the three SWNTs yielding a peak at 4 Å (Figure 4.12a). It is possible to find a few benzene rings near the SWNT surface (Figure 4.12b), but most of the benzene rings are positioned further from the nanotube surfaces, next to the monolayer of tail segments, yielding the largest peak density at ~6 Å. The sulfonate headgroups are for the most parts extended into water (Figure 4.12c). The sodium counterions pack close to the charged of sulfonate headgroups (Figure 4.12d).

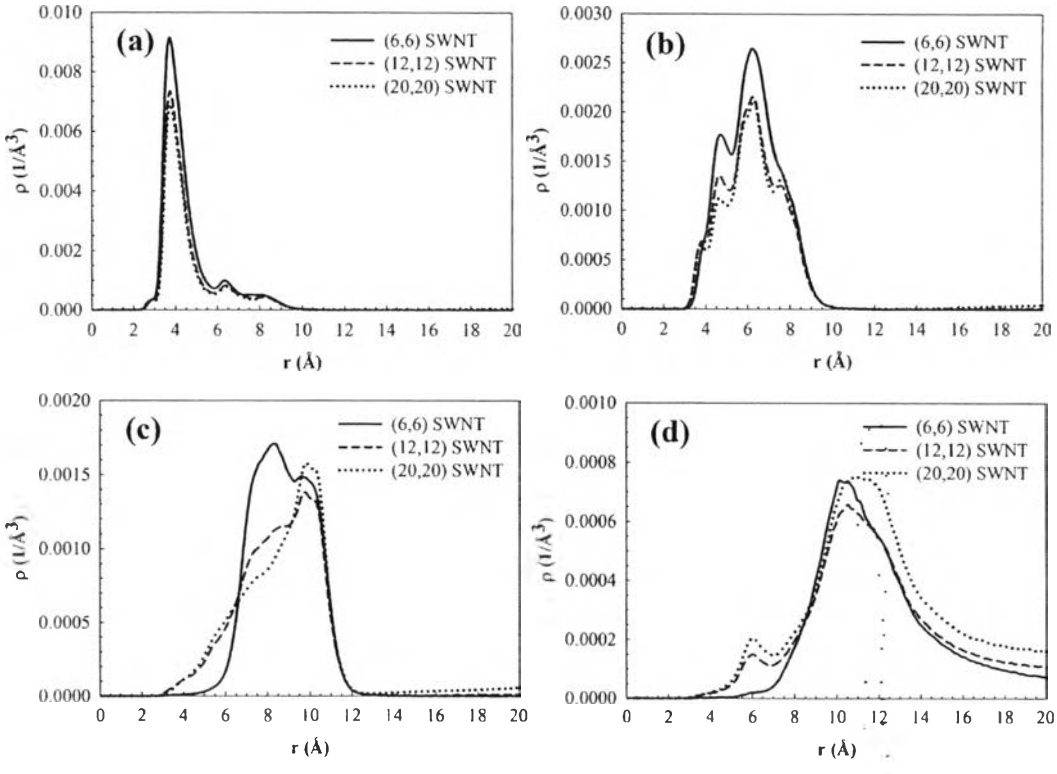

Figure 4.12 Density distribution of (a) tail segments, (b) benzene rings, (c) headgroups, and (d) sodium counterions of branched SDBS relative to the SWNT ("r" is measured radially from the nanotube surface). These results were obtained on the three SWNTs at high surface coverage. The solid, dashed, and dotted lines represent (6,6), (12,12), and (20,20) SWNTs, respectively.

Although it might be a coincidence, it should be pointed out that micellar structures formed at contact with branched SDBS adsorbed on the nanotubes were not observed when branched SDBS were simulated. In summary, the density profiles suggest that as the benzene sulfonate group moves from the end of the alkyl chain to the 5^{th} carbon atom, a change in the aggregate morphology of SDBS on SWNTs can be observed.

4.2.1 Orientation Distribution

To quantify the orientation of branched SDBS adsorbed on the three SWNTs, the probability distribution of the angle between the vector identified by the surfactant tail and the SWNT axis, and that angle between the vector identified by

the benzene sulfonate and the SWNT axis were calculated. For these calculations only the branched SDBS molecules around the SWNT located up to a cutoff distance of 9 (tail) and 12 Å (sulfonate) from the SWNT surface are considered. A schematic describing the two vectors defined by one SDBS molecule is shown in Figure 4.13.

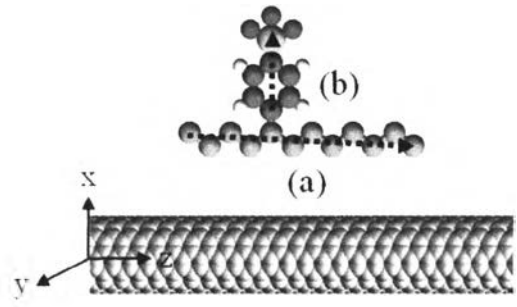

Figure 4.13 The vectors of (a) tail segment and (b) benzene sulfonate group used to calculate the probability distribution of the orientation angle between branched SDBS molecule and the SWNT axis (parallel to the z-axis of the simulation box).

The probability distribution of the orientation of branched SDBS molecules on the various SWNTs is shown in Figure 4.14. The left and right panels are for results observed at low and high surface coverages, respectively. The results show no significant difference between the two surface coverages. The tail segments (Figure 4.14a and 4.14c) tend to form any angle to the SWNTs axis. The benzene sulfonate groups (Figure 4.14b and 4.14d) tend to orient perpendicularly to the SWNT axis, indicating the broad peak at 90°.

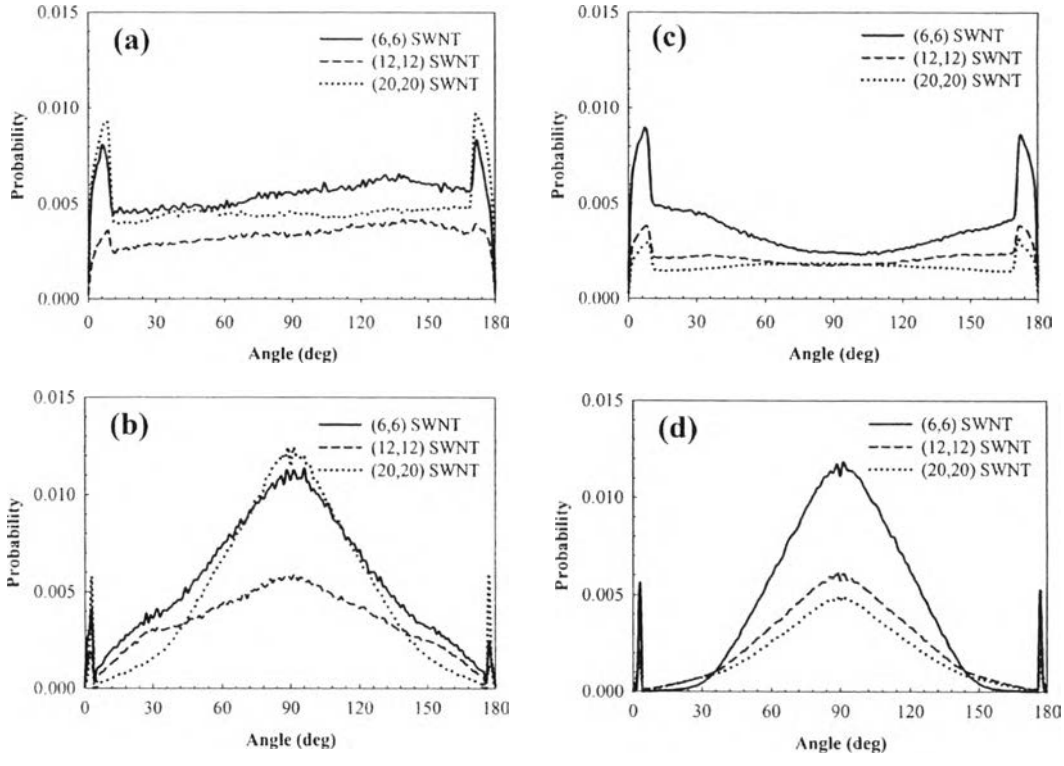

Figure 4.14 Probability distribution of orientation angle formed between the vector of the surfactant tail and the SWNT axis [(a) and (c)] and that between the vector of the benzene sulfonate and the SWNT axis [(b) and (d)]. In the left panels these results were obtained on the three SWNTs at low surface coverage; in the right panels those were obtained at high surface coverage. The solid, dashed, and dotted lines represent (6,6), (12,12), and (20,20) SWNTs, respectively.